Supporting Information

Boosting the Temperature Detection Accuracy of Luminescent Ratiometric Thermometry via a Multifunction Fit Strategy

Leipeng Li,[†] Feng Qin,[*,†] Yuan Zhou,[†] Yangdong Zheng,[‡] Hua Zhao,[§] and Zhiguo Zhang[*,†]

[†]Condensed Matter Science and Technology Institute, [‡]Department of Physics, and [§]School of Materials and Engineering, Harbin Institute of Technology, Harbin 150001, P.R. China

*Corresponding Authors:

E-mail: qinfeng@hit.edu.cn (F. Q.).
E-mail: zhangzhiguo@hit.edu.cn (Z. Z.).

This PDF file includes:

Figure S1. XRD of the phosphors.

Figure S2. Energy level diagrams of Yb^{3+}–Er^{3+} system and the possible UC processes for the $^2H_{11/2}$–$^4I_{15/2}$ and $^4S_{3/2}$–$^4I_{15/2}$ transitions of Er^{3+}, following the 980 nm laser diode irradiation.

Figure S3. $\Delta_{525/550}$ as a function of temperature in the range of 303−783 K.

Figure S4. (a) $\Delta_{525/550}$ as a function of temperature in the range of 303–783 K, as well as the two–function fit result; (b) the temperature errors obtained based on the two–function fit strategy shown in (a).

Discussion S1. Two–function fit strategy.

Figure S5. (a) $\Delta_{525/550}$ as a function of temperature in the range of 303–783 K, as well as the three–function fit result; (b) the temperature errors obtained based on the three–function fit strategy shown in (a).

Discussion S2. Three–function fit strategy.

Figure S6. (a) $\Delta_{525/550}$ as a function of temperature in the range of 303–783 K, as well as the four–function fit result; (b) the temperature errors obtained based on the four–function fit strategy shown in (a).

Discussion S3. Four–function fit strategy.

Figure S7. (a) $\Delta_{525/550}$ as a function of temperature in the range of 303–783 K, as well as the twelve–function fit result; (b) the temperature errors obtained based on the twelve–function fit strategy shown in (a).

Discussion S4. Twelve–function fit strategy.

Figure S8. Comparison of the temperature errors obtained by using the X–function (X=1, 2, 3, 4, 6 and 12) fit methods.

Figure S9. (a) Room temperature upconversion luminescence spectrum of Y_2O_3:Yb^{3+}-Er^{3+} phosphors; (b) luminescence intensity ratio between the $^2H_{11/2}$–$^4I_{15/2}$ and $^4S_{3/2}$–$^4I_{15/2}$ emissions as a function of temperature in the range of 303−583 K.

Figure S10. (a) Luminescence intensity ratio between the $^2H_{11/2}$–$^4I_{15/2}$ and $^4S_{3/2}$–$^4I_{15/2}$ transitions of Er^{3+} (Δ1' and Δ2') as a function of temperature in the range of 303−583 K. Δ1' is the ratio used to obtain the calibration curve and Δ2' is the ratio used to check the calibration curve; (b) and (c) show the results fitted with the one-function and three-function fit strategies; (d) comparison of the temperature errors with the use of the one-function and three-function fit strategies.

Discussion S5. Study on Y_2O_3:Yb^{3+}-Er^{3+} phosphors with the use of same strategy.

Figure S11. Comparison of the pre-exponential factors obtained by using the X–function (X=1, 2, 3, 4, 6 and 12) fit methods.

Figure S12. Comparison of the absolute sensitivities with the use of X-function (X=1, 2, 3, 4, 6 and 12) fit method in the experimental temperature range; (b),(c) and (d) show the comparisons of the absolute sensitivities with the use of X-function (X=1, 2, 3, 4, 6 and 12) fit method at 323, 643 and 763 K, respectively.

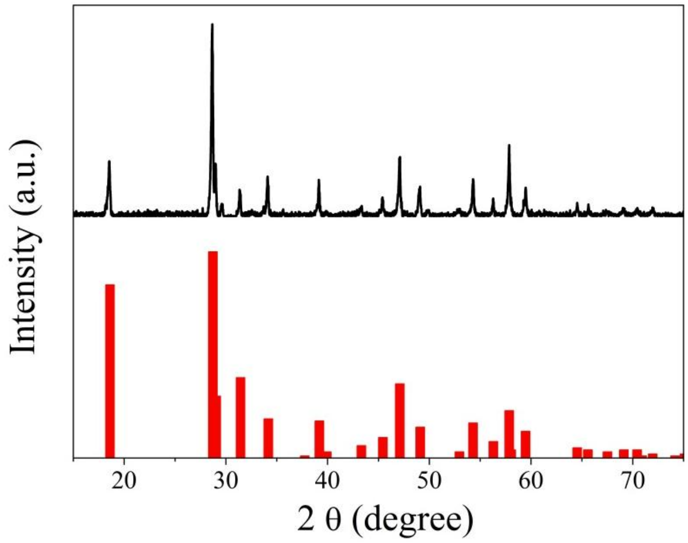

Figure S1. XRD of the phosphors.

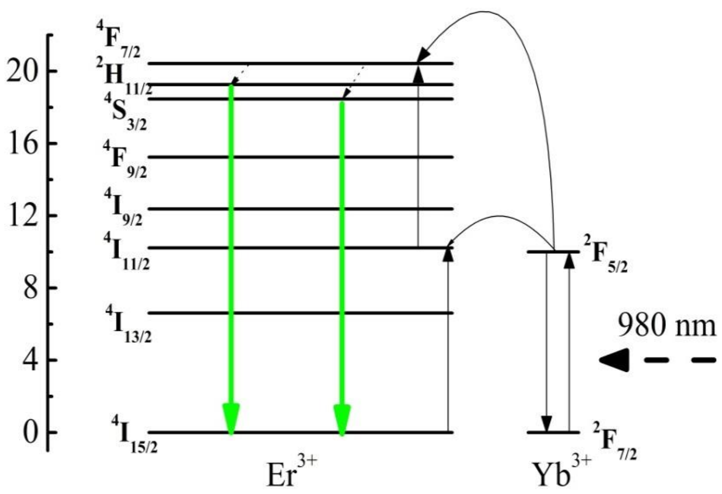

Figure S2. Energy level diagrams of Yb^{3+}–Er^{3+} codoped system and the possible UC processes for the $^{2}H_{11/2}$–$^{4}I_{15/2}$ and $^{4}S_{3/2}$–$^{4}I_{15/2}$ transitions of Er^{3+}, following the 980 nm laser diode irradiation.

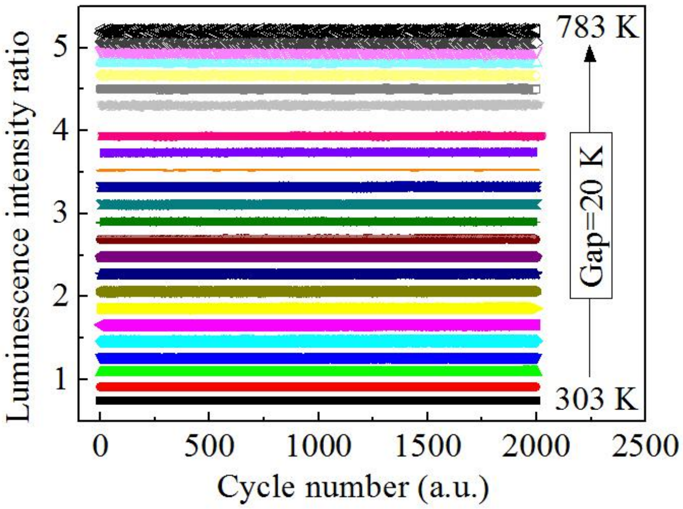

Figure S3. $\Delta_{525/550}$ as a function of temperature in the range of 303−783 K.

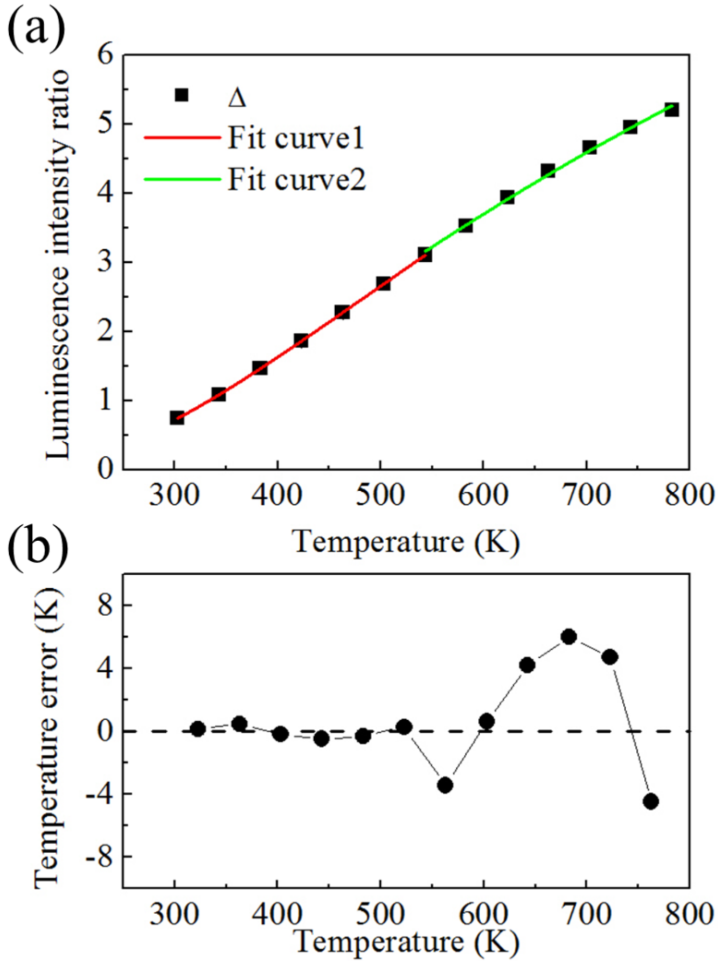

Figure S4. (a) $\mathit{\Delta}_{525/550}$ as a function of temperature in the range of 303–783 K, as well as the two–function fit result; (b) the temperature errors obtained based on the two–function fit strategy shown in (a).

Discussion S1. Two–function fit strategy.

Figure S4(a) presents the fit results using the two–function method in the range of 303–783 K. The specific procedures are described as follows. Firstly, the whole temperature range, that is, 303–783 K, is divided into two small ranges uniformly. Therefore, the two small uniform ranges are 303−543 and 543−783 K, respectively. In each separate temperature range, we can obtain one fit curve with the use of eq (1).

On the basis of the two–function fit method proposed, the following expression could be achieved

$$F = \begin{cases} 18.78\exp(-\dfrac{977.79}{T}) & 303-543\mathrm{K} \\ 16.75\exp(-\dfrac{906.32}{T}), & 543-783\mathrm{K} \end{cases}. \tag{S1}$$

Based on eqs (2) and S1, the temperature errors obtained at 323/363/403/443/483/523/563/603/643/683/723/763 K can be calculated, which are shown in Figure S4(b). The average temperature error over the whole temperature range from 323 to 763 K is 2.11 K. For the conventional one−function fit method, this mean error is calculated to be 3.47 K. Obviously, the two–function fit strategy is able to obtain a more accurate temperature readout than the conventional one.

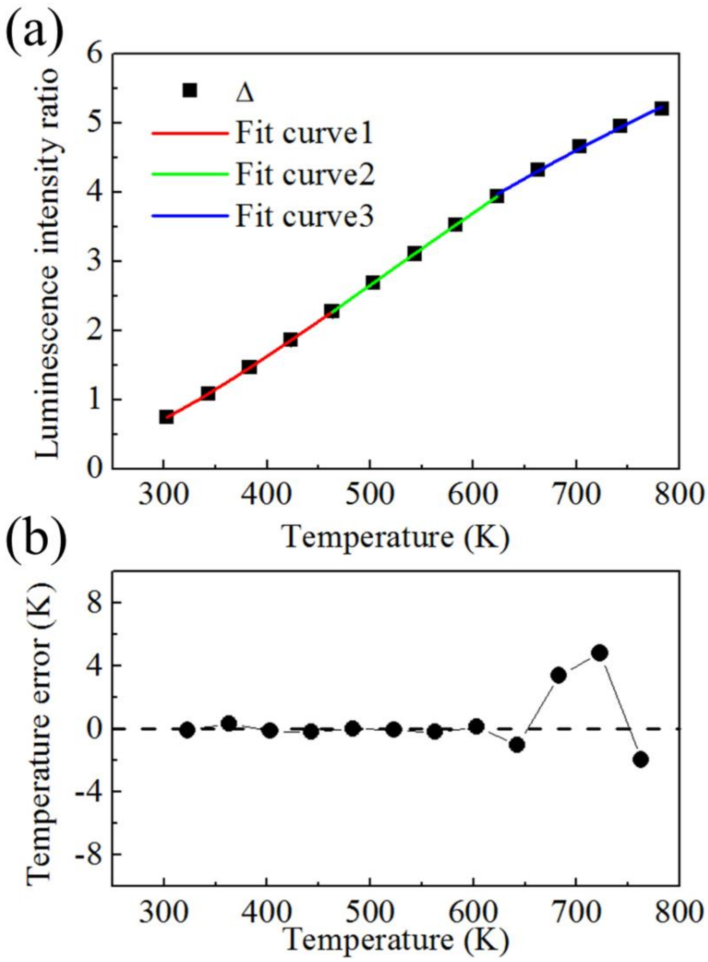

Figure S5. (a) $\Delta_{525/550}$ as a function of temperature in the range of 303–783 K, as well as the three–function fit result; (b) the temperature errors obtained based on the three–function fit strategy shown in (a).

Discussion S2. Three–function fit strategy.

Figure S5(a) presents the fit results using the three–function fit method in the range of 303–783 K. The specific procedures are described as follows. Firstly, the whole temperature range, that is, 303–783 K, is divided into three small ranges uniformly. Therefore, these small uniform ranges are 303−463, 463−623 and 623−783 K, respectively. In each separate temperature range, we can obtain one fit curve with the use of eq (1).

On the basis of the three–function fit method proposed, the following expression could be achieved

$$F=\begin{cases}18.57\exp(-\dfrac{973.50}{T}) & 303-463\mathrm{K}\\ 19.42\exp(-\dfrac{994.70}{T}), & 463-623\mathrm{K}\\ 15.36\exp(-\dfrac{843.47}{T}) & 623-783\mathrm{K}\end{cases}. \tag{S2}$$

Based on eqs (2) and S2, the temperature errors obtained at 323/363/403/443/483/523/563/603/643/683/723/763 K can be calculated, which are shown in Figure S5(b). As can be observed, at relatively low temperatures, the temperature errors are quite small. In contrast, at high temperatures, the temperature errors are relatively large. The average temperature error over the whole temperature range from 323 to 763 K is 1.03 K. For the conventional one−function fit method, this mean error is calculated to be 3.47 K. Obviously, the three–function fit strategy is able to obtain a more accurate temperature readout than the conventional one.

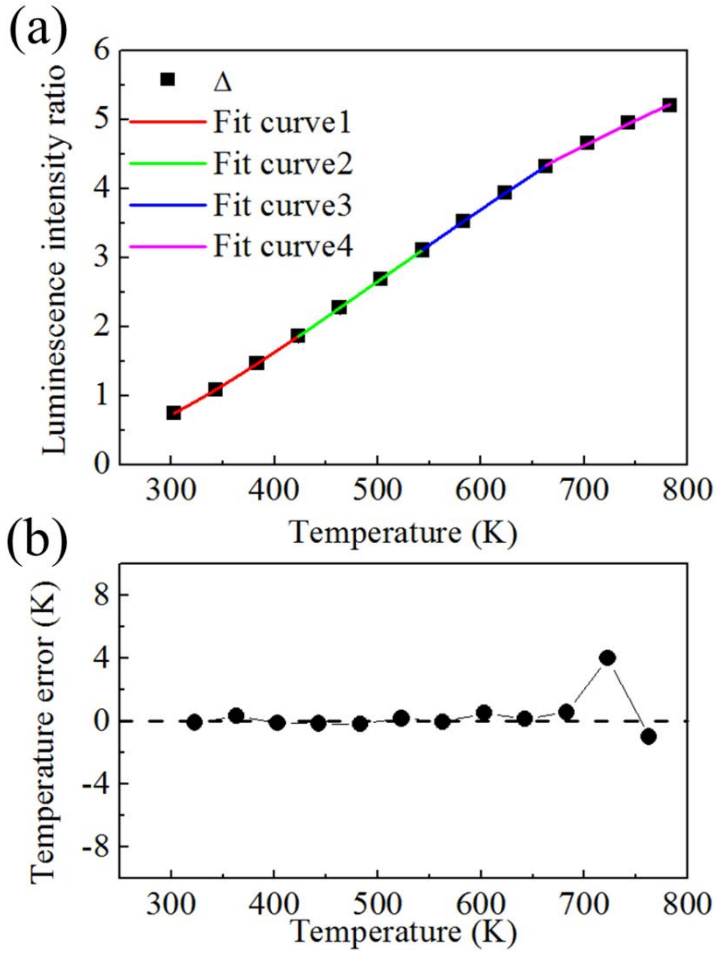

Figure S6. (a) $\Delta_{525/550}$ as a function of temperature in the range of 303–783 K, as well as the four–function fit result; (b) the temperature errors obtained based on the four–function fit strategy shown in (a).

Discussion S3. Four–function fit strategy.

Figure S6(a) presents the fit results using the four–function method in the range of 303–783 K. The specific procedures are described as follows. Firstly, the whole temperature range, that is, 303–783 K, is divided into four small ranges uniformly. Therefore, these small uniform ranges are 303−423, 423−543, 543−663 and 663−783 K, respectively. In each separate temperature range, we can obtain one fit curve with the use of eq (1).

On the basis of the four–function method proposed, the following expression could be achieved

$$F = \begin{cases} 18.56\exp(-\dfrac{973.23}{T}) & 303-423\mathrm{K} \\ 18.99\exp(-\dfrac{983.60}{T}) & 423-543\mathrm{K} \\ 19.25\exp(-\dfrac{990.08}{T}), & 543-663\mathrm{K} \\ 14.49\exp(-\dfrac{800.24}{T}) & 663-783\mathrm{K} \end{cases} \quad \text{(S3)}$$

Based on eqs (2) and S3, the temperature errors obtained at 323/363/403/443/483/523/563/603/643/683/723/763 K can be calculated, which are shown in Figure S6(b). The average temperature error over the whole temperature range from 323 to 763 K is 0.60 K. For the conventional one−function fit method, this mean error is calculated to be 3.47 K. Obviously, the four–function fit strategy is able to obtain a more accurate temperature readout than the conventional one.

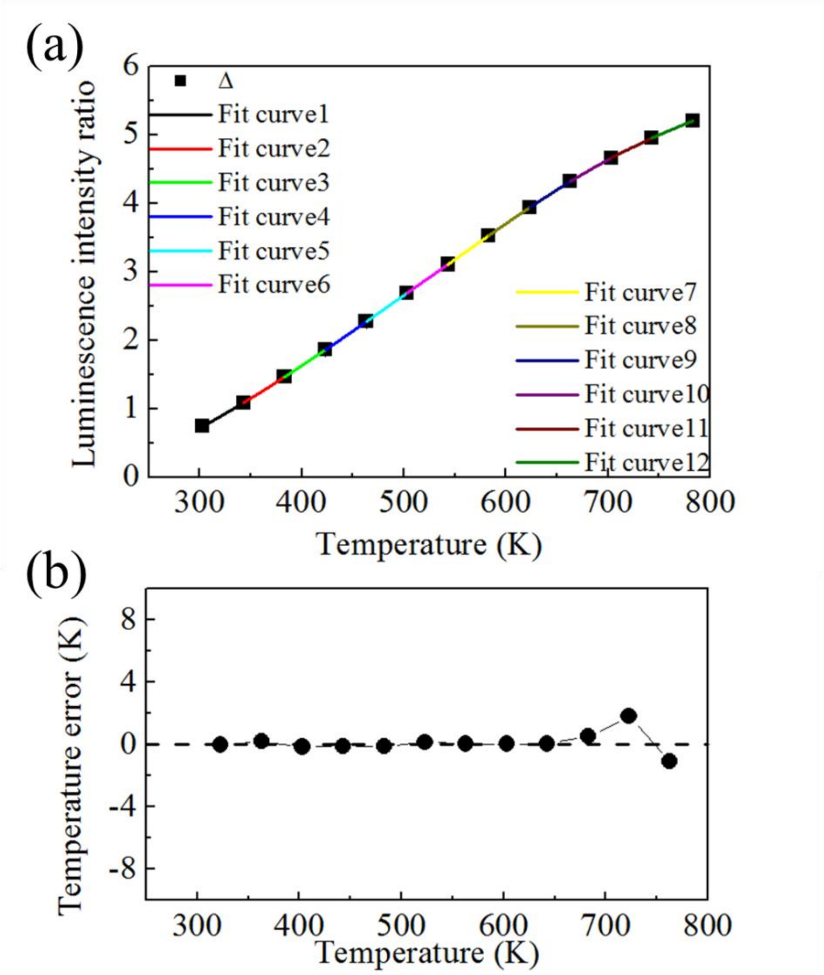

Figure S7. (a) $\Delta_{525/550}$ as a function of temperature in the range of 303–783 K, as well as the twelve–function fit result; (b) the temperature errors obtained based on the twelve–function fit strategy shown in (a).

Discussion S4. Twelve–function fit strategy.

Figure S7(a) presents the fit results using the twelve–function fit method in the range of 303–783 K. The specific procedures are described as follows. Firstly, the whole temperature range, that is, 303–783 K, is divided into twelve small ranges uniformly. Therefore, these small uniform ranges are 303−343, 343−383, 383−423, 423−463, 463−503, 503−543, 543−583, 583−623, 623−663, 663−703, 703−743 and 743−783 K, respectively. In each separate temperature range, we can obtain one fit curve with the use of eq (1).

On the basis of the twelve–function fit method proposed, the following expression could be achieved

$$F=\begin{cases} 19.17\exp(-\dfrac{983.90}{T}) & 303-343\text{K} \\ 18.52\exp(-\dfrac{972.15}{T}) & 343-383\text{K} \\ 18.25\exp(-\dfrac{966.36}{T}) & 383-423\text{K} \\ 18.74\exp(-\dfrac{977.64}{T}) & 423-463\text{K} \\ 19.16\exp(-\dfrac{987.92}{T}) & 463-503\text{K} \\ 19.00\exp(-\dfrac{983.71}{T}) & 503-543\text{K} \\ 19.87\exp(-\dfrac{1008.09}{T}) & 543-583\text{K} \\ 19.54\exp(-\dfrac{998.17}{T}) & 583-623\text{K} \\ 18.37\exp(-\dfrac{959.86}{T}) & 623-663\text{K} \\ 16.43\exp(-\dfrac{885.79}{T}) & 663-703\text{K} \\ 14.44\exp(-\dfrac{794.93}{T}) & 703-743\text{K} \\ 12.88\exp(-\dfrac{710.37}{T}) & 743-783\text{K} \end{cases} \tag{S4}$$

Based on eqs (2) and S4, the temperature errors obtained at 323/363/403/443/483/523/563/603/643/683/723/763 K can be calculated, which are shown in Figure S7(b). The average temperature error over the whole temperature range from 323 to 763 K is 0.35 K. For the conventional one−function fit method, this mean error is calculated to be 3.47 K. Obviously, the twelve–function fit strategy is able to obtain a more accurate temperature readout than the conventional one.

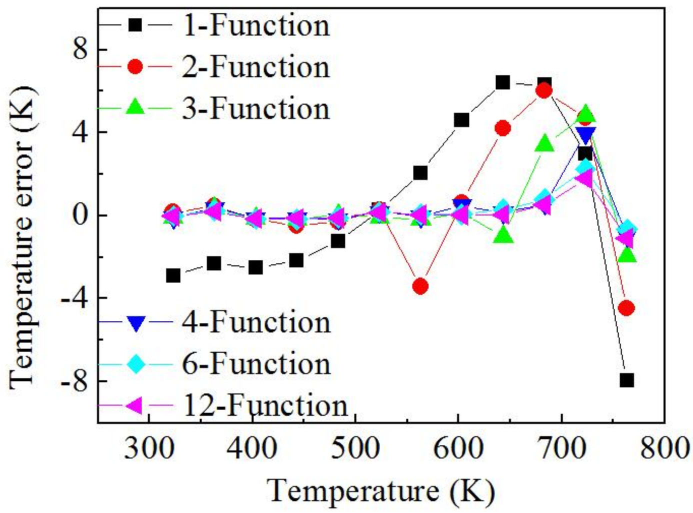

Figure S8. Comparison of the temperature errors obtained by using the X–function (X=1, 2, 3, 4, 6 and 12) fit methods.

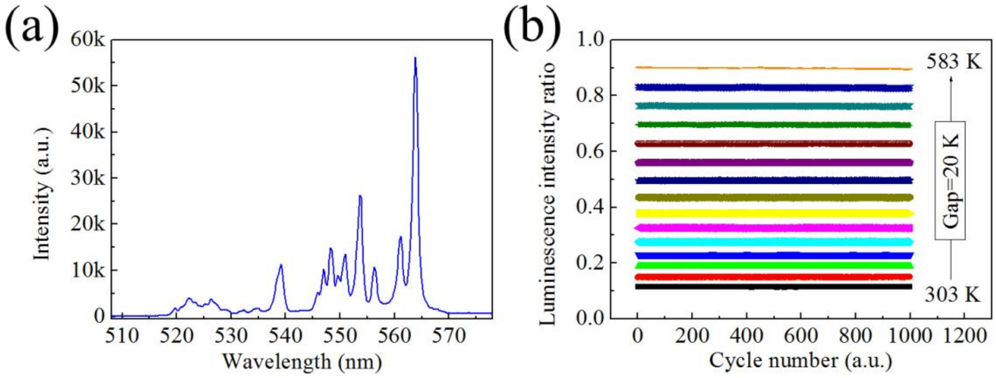

Figure S9. (a) Room temperature upconversion luminescence spectrum of Y_2O_3:Yb^{3+}-Er^{3+} phosphors; (b) luminescence intensity ratio between the $^2H_{11/2}$–$^4I_{15/2}$ and $^4S_{3/2}$–$^4I_{15/2}$ emissions as a function of temperature in the range of 303−583 K.

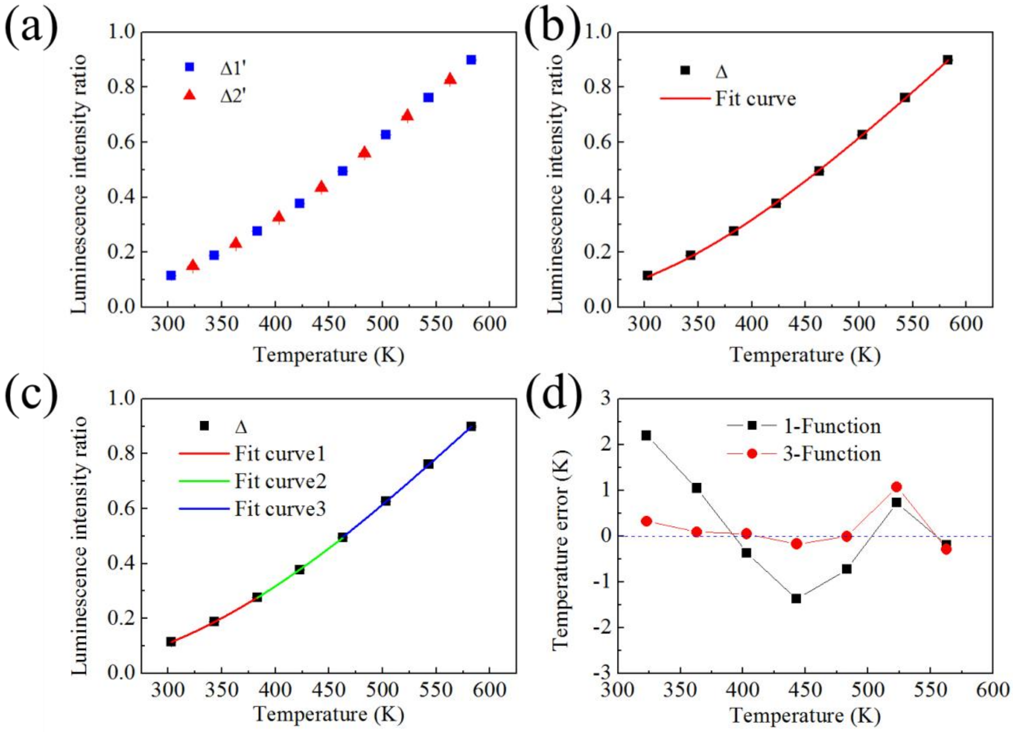

Figure S10. (a) Luminescence intensity ratio between the $^2H_{11/2}$–$^4I_{15/2}$ and $^4S_{3/2}$–$^4I_{15/2}$ transitions of Er^{3+} (Δ1' and Δ2') as a function of temperature in the range of 303−583 K. Δ1' is the ratio used to obtain the calibration curve and Δ2' is the ratio used to check the calibration curve; (b) and (c) show the results fitted with the one-function and three-function fit strategies; (d) comparison of the temperature errors with the use of the one-function and three-function fit strategies.

Discussion S5. Study on Y_2O_3:Yb^{3+}-Er^{3+} phosphors with the use of same strategy.

Figure S9(a) presents the room temperature upconversion luminescence spectrum of Y_2O_3:Yb^{3+}-Er^{3+} phosphors. The spectral ranges in 500-540 nm and 545-570 nm could be ascribed to the $^2H_{11/2}$–$^4I_{15/2}$ and $^4S_{3/2}$–$^4I_{15/2}$ transitions, respectively. Figure S9(b) and 10(a) show the luminescence intensity ratio Δ between the $^2H_{11/2}$–$^4I_{15/2}$ and $^4S_{3/2}$–$^4I_{15/2}$ emissions as a function of temperature in the range of 303−583 K. In Figure 10(a), the ratios marked as blue squares are obtained at 303, 343, 383, 423, 463, 503, 543 and 583 K, which are used to obtain the calibration curve. While the red triangles, obtained at 323, 363, 403, 443, 483, 523 and 563 K, are the measured luminescence intensity ratios used to check the calibration curves. Figure S10(b) presents the fit result with the use of one-function fit method. The specific expression is

$$\Delta = 8.64\exp(-\frac{1320.09}{T}) . \tag{S5}$$

In contrast, Figure S10(c) presents the fit result with the use of three-function fit method. The specific expression is

$$\Delta = \begin{cases} 7.79\exp(-\frac{1279.01}{T}) & 303-383\text{K} \\ 8.17\exp(-\frac{1298.91}{T}) & 383-463\text{K} \\ 8.88\exp(-\frac{1335.29}{T}) , & 463-583\text{K} . \end{cases} \tag{S6}$$

Figure S10(d) shows the comparison of the calculated temperature errors with the use of one-function and three-function fit strategies. The average temperature errors for these two strategies are calculated to be 0.94 and 0.28 K, respectively. Obviously, the three-function fit strategy is able to obtain a more accurate temperature readout than the conventional one.

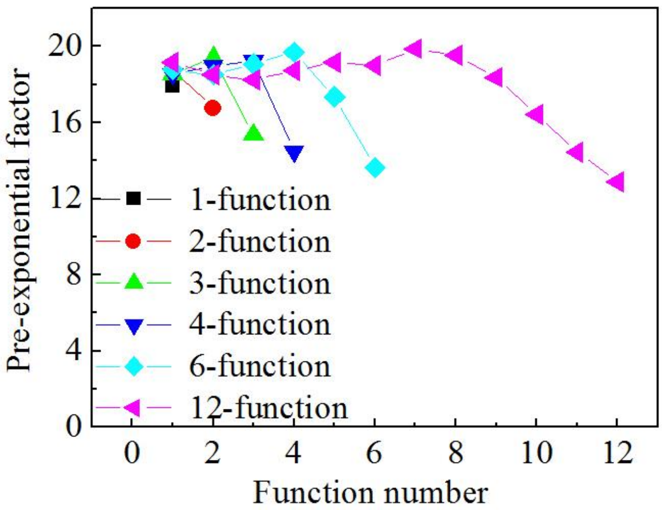

Figure S11. Comparison of the pre-exponential factors obtained by using the X–function (X=1, 2, 3, 4, 6 and 12) fit methods.

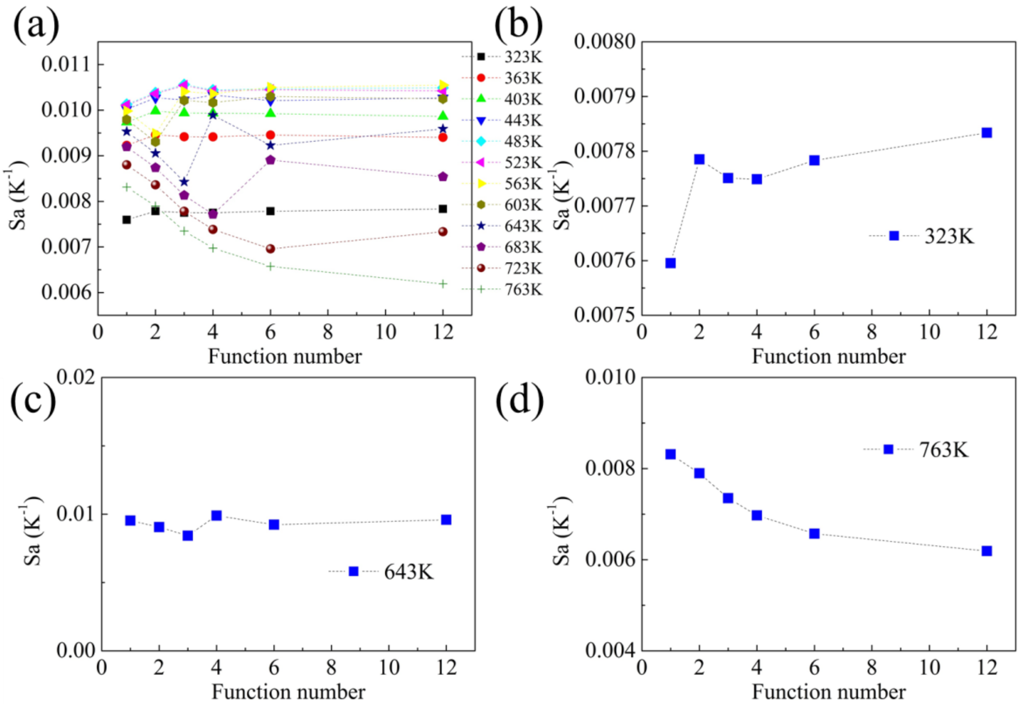

Figure S12. Comparison of the absolute sensitivities with the use of X-function (X=1, 2, 3, 4, 6 and 12) fit method in the experimental temperature range; (b),(c) and (d) show the comparisons of the absolute sensitivities with the use of X-function (X=1, 2, 3, 4, 6 and 12) fit method at 323, 643 and 763 K, respectively.